



**HAL**  
open science

## Haptic control of the parallel robot Orthoglide

Philippe Lemoine, Pierre-Philippe P Robet, Damien Chablat, Yannick Aoustin, Maxime Gautier

► **To cite this version:**

Philippe Lemoine, Pierre-Philippe P Robet, Damien Chablat, Yannick Aoustin, Maxime Gautier. Haptic control of the parallel robot Orthoglide. 24ème Congrès Français de Mécanique, CFM 2019, Aug 2019, Brest, France. hal-02264290

**HAL Id: hal-02264290**

**<https://hal.science/hal-02264290>**

Submitted on 6 Aug 2019

**HAL** is a multi-disciplinary open access archive for the deposit and dissemination of scientific research documents, whether they are published or not. The documents may come from teaching and research institutions in France or abroad, or from public or private research centers.

L'archive ouverte pluridisciplinaire **HAL**, est destinée au dépôt et à la diffusion de documents scientifiques de niveau recherche, publiés ou non, émanant des établissements d'enseignement et de recherche français ou étrangers, des laboratoires publics ou privés.

# Haptic control of the parallel robot *Orthoglide*

**P. LEMOINE<sup>a</sup>, P. P. ROBET<sup>a</sup>, M. GAUTIER<sup>a</sup>, D. CHABLAT<sup>a</sup>,  
Y. Aoustin<sup>a</sup>**

a. Laboratoire des Sciences du Numérique de Nantes, UMR CNRS 6004 + email (12)  
1 rue de la Noë, BP 92101 F-44321 Nantes Cedex 3, France  
Ecole Centrale de Nantes, Université de Nantes,  
philippe.lemoine@ec-nantes.fr, Pierre-philippe.Robet@univ-nantes.fr,  
Maxime.Gautier@univ-nantes.fr, damien.chablat@cnr.fr,  
and Yannick.Aoustin@univ-nantes.fr

## Résumé :

*Cet article traite de la conception d'une commande de rétroaction haptique du robot parallèle Orthoglide pour effectuer des tâches de co-manipulation. Nous rappelons les différents modèles géométrique, cinématique et dynamique de Orthoglide. A partir de la mesure de la force d'interaction entre l'opérateur humain et l'effecteur final du robot, une trajectoire de référence de la plate-forme est calculée dans l'espace Cartésien. Cette trajectoire de référence est projetée dans l'espace articulaire pour obtenir la trajectoire de référence des variables actives de l'articulation linéaire. Un modèle dynamique simplifié est proposé et justifié pour concevoir une loi de commande de couple calculée des articulations linéaires actionnées dans l'espace articulaire. L'étude théorique et les résultats expérimentaux sur Orthoglide montrent comment les robots industriels rigides classiques avec une bande passante en boucle fermée à vitesse et position élevées peuvent être adaptés à des tâches de co-manipulation très efficaces. Cet article offre des perspectives intéressantes pour de nombreuses applications fondées sur l'interaction robot/humain dans un environnement industriel.*

## Abstract :

*This paper addresses the design of a haptic feedback control of the parallel robot Orthoglide to perform co-manipulation tasks. We recall the different geometric, kinematic and dynamic models of Orthoglide. From the measurement of the interaction force between the human operator and the end effector of the robot a reference trajectory of the platform is computed in the Cartesian space. This reference trajectory is projected in the joint space to obtain the reference trajectory of the active linear joint variables. A simplified dynamic model is proposed and justified to design a computed torque control law of the active linear joints in the joint space. Theoretical study and experimental results on the Orthoglide show how classical rigid industrial robots with high velocity and position closed loop bandwidth can be adapted for very efficient co-manipulation tasks. This paper offers interesting perspectives to numerous applications based on the interaction robot/human in an industrial environment.*

**Mots clés : Commande haptique, commande en effort, transparence, co-manipulation, interaction homme-robot, asservissement, espace opérationnel, espace articulaire, modèle réduit, robot parallèle.**

**Keywords : Haptic control, force control, transparency, co-manipulation, human-robot interaction, feedback, operational space, joint space, reduced model, parallel robot.**

## Nomenclature

- m : Meter.
- Kg : Kilogram.
- s : Second.
- N : Newton.
- Hz : Hertz.
- rad : Radian.
- dB : Decibel.
- ${}^0\mathbf{R}_p$  : Reference frame.
- $m_p$  (Kg) : Mass of the platform of *Orthoglide*.
- $g = 9.81 \text{ m.s}^{-2}$  : Constant gravity.
- ${}^0\mathbf{g} = \begin{pmatrix} 0 & 0 & g \end{pmatrix}^\top$  : Vector of acceleration of gravity, referred to reference frame  ${}^0\mathbf{R}_p$ .
- $\mathbf{q}_a(3 \times 1) = \begin{pmatrix} \rho_1 & \rho_2 & \rho_3 \end{pmatrix}^\top$  : Vector of the actuated linear joint variables, associated to the linear actuators of *Orthoglide*.
- $\mathbf{q}_{na}(6 \times 1)$  is the vector of the joint variables not actuated of *Orthoglide*.
- $\dot{\mathbf{q}}_a(3 \times 1) = \begin{pmatrix} \dot{\rho}_1 & \dot{\rho}_2 & \dot{\rho}_3 \end{pmatrix}^\top$  : Time derivative of  $\mathbf{q}_a$ .
- $\dot{\mathbf{q}}_{na}(6 \times 1)$  : Time derivative of  $\mathbf{q}_{na}$ .
- $\ddot{\mathbf{q}}_a(3 \times 1) = \begin{pmatrix} \ddot{\rho}_1 & \ddot{\rho}_2 & \ddot{\rho}_3 \end{pmatrix}^\top$  : Time derivative of  $\dot{\mathbf{q}}_a$ .
- $\ddot{\mathbf{q}}_{na}(6 \times 1)$  : Time derivative of  $\dot{\mathbf{q}}_{na}$ .
- $\mathbf{q}(9 \times 1) = \begin{pmatrix} q_a & q_{na} \end{pmatrix}^\top$  : Vector of the generalized coordinates of *Orthoglide*.
- $\dot{\mathbf{q}}(9 \times 1) = \begin{pmatrix} \dot{q}_a & \dot{q}_{na} \end{pmatrix}^\top$  : Time derivative of  $\mathbf{q}$ .
- $\ddot{\mathbf{q}}(9 \times 1) = \begin{pmatrix} \ddot{q}_a & \ddot{q}_{na} \end{pmatrix}^\top$  : Time derivative of  $\dot{\mathbf{q}}$ .
- ${}^0\mathbf{P}_p(3 \times 1) = \begin{pmatrix} x_p & y_p & z_p \end{pmatrix}^\top$  : Vector of the Cartesian position of the platform of *Orthoglide* with respect to  ${}^0\mathbf{R}_p$ .
- ${}^0\mathbf{V}_p(3 \times 1) = \begin{pmatrix} \dot{x}_p & \dot{y}_p & \dot{z}_p \end{pmatrix}^\top$  : Vector of the Cartesian velocity of the platform of *Orthoglide* with respect to  ${}^0\mathbf{R}_p$ .
- ${}^0\dot{\mathbf{V}}_p(3 \times 1) = \begin{pmatrix} \ddot{x}_p & \ddot{y}_p & \ddot{z}_p \end{pmatrix}^\top$  : Vector of the Cartesian acceleration of the platform of *Orthoglide* with respect to  ${}^0\mathbf{R}_p$ .

## 1 Introduction

A lot of avances in robotic technologies have led to the emergence of new applications that involve physical interactions between human and robots. For these new applications, it is necessary to control the position and interaction forces between the robot effector and the human. Humans react to unforeseen changes in daily life and perform skillful manipulation tasks. Today's rigid industrial robots have good repeatability, which is in the order of a hundredth of a millimeter at the end effector, and high dynamics of the drive chain. Its bandwidth can then reach several tens of hertz [1]. These characteristics make it possible to obtain fast and precise movements of the robots. It is then possible to extend the applications

of these robots to co-manipulation and teleoperation thanks to the haptic feedback. Several contributions to strengthen the interaction between the robot and the human can be thus identified. For example Lie *et al* [2] formulated a human-guided co-manipulation problem to take advantages of both human knowledge and the robot's capacities in a stable manner. The force amplification case in co-manipulation with an industrial robot is addressed by Lamy *et al* [3] with presented theoretical and experimental results. Peternel *et al* [4] propose to manage muscle fatigue in human-robot co-manipulation. A machine learning technique is used to enable online predictions of muscle forces in different arm configurations and endpoint interaction forces. Then a fatigue management system can operate online. Despite the remarkable existing applications that we can observe, there are few industrial application interactions between human and robots. There are still open problems. How to design an efficient haptic feedback with an industrial multi-body robot?

The purpose of this paper is to prove that it is possible to achieve a haptic feedback with a parallel robot called *Orthoglide* [5]. This robot has three prismatic joints that allow high Cartesian accelerations of the effector as well as uniform precision in the work area. To perform a haptic feedback the measure of the motor currents is an attractive idea to avoid the use of a force sensor. However the drive chains of the industrial robots generally include mechanical reducers, mechanical coupling systems between several drive chains, or motion conversion mechanisms. All these mechanical systems introduce friction that can absorb up to 80% of the mechanical power [6]. These frictions depend on the temperature, the humidity of the environment, the mechanical constraints applied to the robot. Finally, these drive chains are often not very transparent. This means that an external force applied to the effector must be high to obtain a movement of the robot. These technological characteristics mean that a fine control of the robot's force on its environment or a co-manipulation control are not possible by simply measuring the motor currents. The addition of a force sensor is necessary to take into account the interaction robot/environment or man/robot. Thus the effector of *Orthoglide* (a platform) is equipped with a force sensor. Two feedback controls are defined for *Orthoglide*. The first one, which controls the joint variables, is performed with a linearizing control law, the well-known "computed torque" method. The new input consists of the addition of a desired acceleration and a correction in position, velocity in order to asymptotically cancel the position error, whose behavior is governed by a linear differential equation. Disturbances such as an unknown stiffness of the environment are mainly rejected by the feedback control of the joint variables. Unexpected collisions of the robot with the environment must also be managed by this feedback control of the joint variables. It must therefore be able to trigger an emergency stop. The second feedback control is dedicated to haptic feedback. It includes the effector, the sensor and the environment or user with whom it interacts. The bandwidth of this haptic feedback control is lower than that of the feedback velocity and position control of the joint rigid variables. The bandwidths of the joint control as well as the internal current loop of the drives are such that their actions can be considered equivalent to that of gain compared to the haptic feedback. For the haptic feedback control the input is the desired force, the output is the force measured by the force sensor. The difference between these two forces is calculated and a dissipative force is added. The net force is converted into a Cartesian acceleration by applying the equivalence, force / (mass acceleration) with a variable gain. This Cartesian acceleration is integrated to define a velocity and position references in the operating space. These Cartesian reference trajectories are projected into the joint space to obtain the acceleration, velocity and position references of the feedback control of the joint variables. Different applications can be considered for the haptic feedback as follows [7] :

- For a man/robot collaboration task, the transparency of the robot is required. The operator must not feel the inertial forces of the robot to be able to guide the effector freely.

- For a force control task, the difference between the desired force and the measured force is converted into a velocity reference in the operating space. The velocity/force conversion gain is a stiffness parameter whose choice is such that it ensures the stability of the hybrid feedback control. If the difference between the desired force and the measured force is converted into an acceleration reference, a dissipative virtual force must be added to the force applied by the environment or operator. This dissipative force ensures that the robot stops when the environment or the operator no longer exerts any action on the force sensor. This last method method is applied in our case.

The perspective of this work is to perform a teleoperation task between *Orthoglide* and another parallel robot with three prismatic joints and a cardan link composed of the revolute joints.

The rest of the paper is outlined as follows. Section 2 is devoted to the presentation of *Orthoglide*, its geometric, kinematic, and dynamic models. The statement of the problem is developed in section 3 to explain our strategy. Our experimental results are presented in section 4. Section 5 offers our conclusion and perspectives.

## 2 The parallel robot *Orthoglide*

### 2.1 General presentation of *Orthoglide*

The parallel robot *Orthoglide* has three parallel *PRPaR* identical legs, see Figure 1 a). The *P*, *R*, and *Pa* stand for Prismatic, Revolute and Parallelogram joint, respectively. Each leg has one active prismatic joint and six passive revolute joints, see [5] and [8]. The interesting features of the *Orthoglide* are a regular Cartesian workspace shape, which is shown Figure 1c and uniform performances in all directions, and good compactness. Robot *Orthoglide* was designed for high-speed machining. The machine reaches a tool velocity of 1.2 m/s and an acceleration of 20 m/s<sup>2</sup> at the isotropic configuration. The bandwidth of the actuator chain, taking into account its electromagnetic constant, is 243 Hz. To avoid any mechanical vibration we limit it to 15 Hz. However, this value is still important in relation to the dynamics of the human gesture during a co-manipulation task. For human gesticulatory, it is difficult for the hand to oscillate at greater than 4.5 Hz, see [9]. Furthermore now with this limitation *Orthoglide* satisfies the ISO standard 10218 and in particular the following constraint : the effector velocity should not exceed 0.25 m/s, see [10]. The motors transform a revolute motion in a translation motion through a ball screw. Each actuator is equipped of an encoder sensor that the resolution at the shaft output of the ball screw is equal to  $2.5 \cdot 10^{-6}$  m per encoder point. The results of the identification of joint drive gains and dynamic parameters of *Orthoglide* can be found in [11].

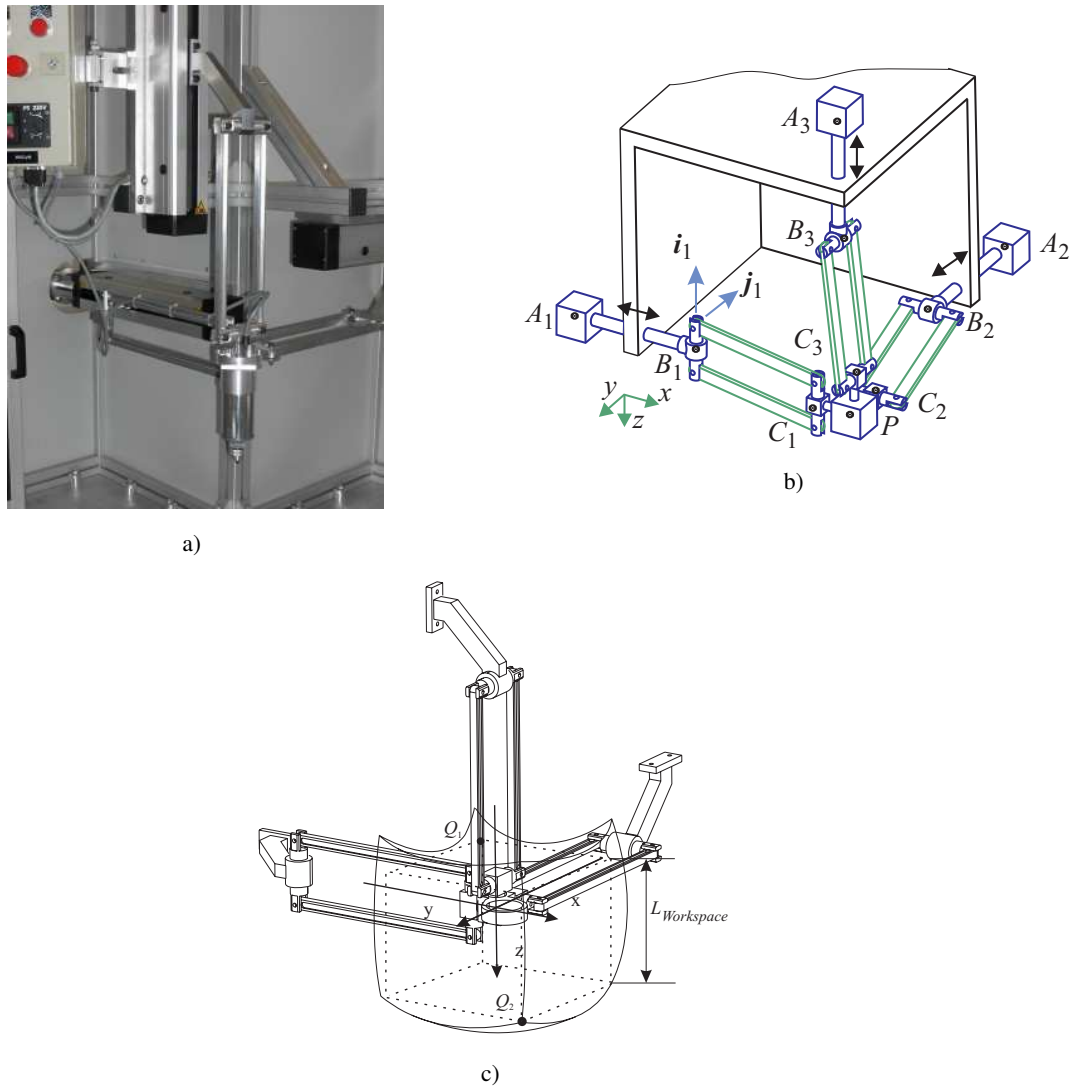


FIGURE 1: a) *Orthoglide*'s photography, b) Geometric design of *Orthoglide*, c) Workspace limits of *Orthoglide*.

## 2.2 Geometric modeling

Let us introduce the following constraint equations linking the actuator positions  $\mathbf{q}_a$  with the Cartesian positions  ${}^0\mathbf{P}_p$  of the platform :

$$\begin{aligned} (x_p - \rho_1)^2 + y_p^2 + z_p^2 &= L^2 \\ x_p^2 + (y_p - \rho_2)^2 + z_p^2 &= L^2 \\ x_p^2 + y_p^2 + (z_p - \rho_3)^2 &= L^2 \end{aligned} \quad (1)$$

with  $L$  is the link lengths such that  $L = C_i B_i$ ; the linear joint variables are equal to  $\rho_i = A_i B_i$  ( $i = 1, 2, 3$ ), see Figure 1 b). The inverse geometric model (IGM) defines the actuator positions  $\mathbf{q}_a = \begin{pmatrix} \rho_1 & \rho_2 & \rho_3 \end{pmatrix}^\top$  as function of the Cartesian positions  ${}^0\mathbf{P}_p$ . With reference to Figure 1 b) IGM is as

follows :

$$\begin{aligned}\rho_1 &= x_p + \sqrt{1 - y_p^2 - z_p^2} \\ \rho_2 &= y_p + \sqrt{1 - x_p^2 - z_p^2} \\ \rho_3 &= z_p + \sqrt{1 - x_p^2 - y_p^2}\end{aligned}\quad (2)$$

### 2.3 Inverse kinematic model of *Orthoglide*

The following kinematic models (*IKM*) are introduced in [12].

1. The inverse kinematic model defining the velocity vector  $\dot{\mathbf{q}}_a = \begin{pmatrix} \dot{\rho}_1 & \dot{\rho}_2 & \dot{\rho}_3 \end{pmatrix}^\top$  can be written as :

$$\dot{\mathbf{q}}_a = {}^0\mathbf{J}_p^{-1} {}^0\mathbf{V}_p \quad (3)$$

Here  ${}^0\mathbf{J}_p^{-1}$  is the inverse Jacobian matrix of *Orthoglide*. Its expression is as follows :

$${}^0\mathbf{J}_p^{-1} = \begin{pmatrix} 1 & -\frac{x_p}{\rho_1 - x_p} & -\frac{x_p}{\rho_1 - x_p} \\ -\frac{y_p}{\rho_2 - y_p} & 1 & -\frac{y_p}{\rho_2 - y_p} \\ -\frac{z_p}{\rho_3 - z_p} & -\frac{z_p}{\rho_3 - z_p} & 1 \end{pmatrix} \quad (4)$$

This matrix is always regular in the working space.

2. The second order direct kinematic model of *Orthoglide* gives the Cartesian platform acceleration  ${}^0\dot{\mathbf{V}}_p$  as function of the joint acceleration vector  $\ddot{\mathbf{q}}_a = \begin{pmatrix} \ddot{\rho}_1 & \ddot{\rho}_2 & \ddot{\rho}_3 \end{pmatrix}^\top$  of the active joint variables and the velocity vector  $\dot{\mathbf{q}}_a$  as follows :

$${}^0\dot{\mathbf{V}}_p = {}^0\mathbf{J}_p\ddot{\mathbf{q}}_a + {}^0\dot{\mathbf{J}}_p\dot{\mathbf{q}}_a \quad (5)$$

3. The second order inverse kinematic model of *Orthoglide* can be deduced from the time derivative of (3) as follows :

$$\ddot{\mathbf{q}}_a = {}^0\dot{\mathbf{J}}_p^{-1} {}^0\mathbf{V}_p + {}^0\mathbf{J}_p^{-1} {}^0\dot{\mathbf{V}}_p \quad (6)$$

### 2.4 Dynamic model of *Orthoglide*

The Cartesian platform acceleration  ${}^0\dot{\mathbf{V}}_p$  can be calculated with the direct dynamic model (*DDM*) as follows, [12], [13], and [8] :

$${}^0\dot{\mathbf{V}}_p = \mathbf{A}(\mathbf{q})_{robot}^{-1} [{}^0\mathbf{J}_p^{-\top} \Gamma - \mathbf{h}(\mathbf{q}, \dot{\mathbf{q}})_{robot}] \quad (7)$$

Here

- $\mathbf{A}(\mathbf{q})_{robot}^{-1} = \sum_{i=1}^3 [\mathbf{A}(\mathbf{q})_{ix}^{-1}] + \mathbf{I}_{3m_p}$  is the inertia matrix ( $3 \times 3$ ) of *Orthoglide* with its movable platform.
- $\mathbf{A}(\mathbf{q})_{robot}$  is the inertia matrix ( $3 \times 3$ ) of *Orthoglide* with its movable platform.  $\mathbf{A}(\mathbf{q})_{robot}$  is a positive definite matrix and therefore always invertible.
- $\mathbf{h}(\mathbf{q}, \dot{\mathbf{q}})_{robot}$  is the vector of Coriolis, gravitation and centrifuge effects ( $3 \times 3$ ) of *Orthoglide* with its movable platform.



- $\Gamma = [\Gamma_1 \ \Gamma_2 \ \Gamma_3]^\top$  is the force vector of the actuators at the output of the ball screws of the actuators.

Taken into account that there is no rotation of the platform its dynamic equation can be written as follows :

$${}^0\mathbf{F}_p = {}^0\dot{\mathbf{V}}_p m_p - {}^0\mathbf{g} m_p, \quad (8)$$

where  ${}^0\mathbf{F}_p$  is the vector, which represents the net external force applied on the platform. Substituting (5) into (7) yields :

$${}^0\mathbf{J}_p^\top \mathbf{A}(\mathbf{q})_{robot} ({}^0\mathbf{J}_p \ddot{\mathbf{q}}_a + {}^0\dot{\mathbf{J}}_p \dot{\mathbf{q}}_a) + {}^0\mathbf{J}_p^\top \mathbf{h}(\mathbf{q}, \dot{\mathbf{q}})_{robot} = \Gamma \quad (9)$$

Equation (9) represents the inverse dynamique model in the joint space.

## 3 Problem statement

### 3.1 In the Cartesian space

The objective is to generate a trajectory of the platform *Orthoglide* in reaction to a force applied by the human operator, in order to perform the most accurate co-manipulation task possible. The robot must therefore not resist the movement that results from interaction with human. This interaction must therefore be transparent to the operator. A force sensor, ATI Delta SI-165-15 from Schunk company, is attached to the platform of *Orthoglide*. This force sensor allows us to measure the three components along  $x$ -axis,  $y$ -axis, and  $z$ -axis of the force, which is applied by the operator. These three force components are measured with a sampling frequency  $f_s = \frac{1}{\Delta}$ , which is equal to 6 kHz. The measured data are filtered by using a Butterworth filter with a cut-off frequency equal to 25 Hz. To define the desired Cartesian acceleration of the platform let us introduce two virtual terms.

First for safety it is important that the platform stops when no effort is applied to it by the operator. It is also important that when interacting between the robot and the operator, the latter, when applying a force to the platform, feels an inertial effect of the robot in order to better modulate the acceleration of the platform. This makes it easier for the operator to achieve the desired platform positioning at any time during the co-manipulation task. Therefore we introduce the following virtual force along each axis such as :

$$F_l \text{ virtual} = \begin{cases} \mu \text{ sign}(\dot{l}_p) & \text{if } \dot{l}_p \neq 0 \\ \mu \text{ sign}(F_l) & \text{if } |F_l| \geq \mu \text{ and } \dot{l}_p = 0 \\ F_l & \text{if } |F_l| < \mu \text{ and } \dot{l}_p = 0 \end{cases} \quad (10)$$

with  $l \in x, y, z$  and  $\mu = 0.8$  N, and where  $F_l$  is the force measured by the force sensor along the  $l$ -axis.

Secondly let us also introduce a virtual mass  $m_{virtual}$  as parameter to deduce an acceleration from an effort. By using these previous parameters we calculate the desired Cartesian acceleration of the platform as follows :

$$\ddot{x}_p = \frac{F_x - F_x \text{ virtual}}{m_{virtual}}, \quad \ddot{y}_p = \frac{F_y - F_y \text{ virtual}}{m_{virtual}}, \quad \ddot{z}_p = \frac{F_z - F_z \text{ virtual}}{m_{virtual}}. \quad (11)$$

The Cartesian acceleration is considered constant during the sampling period  $\Delta$ . So the Cartesian motion is uniformly along each direction  $x$ ,  $y$ , and  $z$  during the sampling period  $\Delta$ . Therefore the desired Cartesian velocity and position vectors are expressed as follows where at each sampling time  $t_k = k\Delta$ ,  $k = 0, \dots, n$  the new the components of the Cartesian velocity vector  ${}^0\mathbf{V}_p$  and of the

Cartesian position vector  ${}^0\mathbf{P}_p$  will be as follows :

$$\begin{aligned}\dot{x}_p(t_k) &= \ddot{x}_p(t_k)\Delta + \dot{x}_p(t_{k-1}) \\ \dot{y}_p(t_k) &= \ddot{y}_p(t_k)\Delta + \dot{y}_p(t_{k-1}) \\ \dot{z}_p(t_k) &= \ddot{z}_p(t_k)\Delta + \dot{z}_p(t_{k-1})\end{aligned}\quad (12)$$

and

$$\begin{aligned}x_p(t_k) &= \ddot{x}_p(t_k)\frac{\Delta^2}{2} + \dot{x}_p(t_{k-1})\Delta + x_p(t_{k-1}) \\ y_p(t_k) &= \ddot{y}_p(t_k)\frac{\Delta^2}{2} + \dot{y}_p(t_{k-1})\Delta + y_p(t_{k-1}) \\ z_p(t_k) &= \ddot{z}_p(t_k)\frac{\Delta^2}{2} + \dot{z}_p(t_{k-1})\Delta + z_p(t_{k-1})\end{aligned}\quad (13)$$

with  ${}^0\mathbf{V}_p(t_{-1}) = 0$ ,  ${}^0\mathbf{P}_p(t_{-1}) = 0$ , and the following initial conditions  ${}^0\mathbf{V}_p(t_0) = \mathbf{V}_0$  and  ${}^0\mathbf{P}_p(t_0) = \mathbf{P}_0$ . The variables  $\ddot{x}_p$ ,  $\ddot{y}_p$ , and  $\ddot{z}_p$  are those calculated with (11).

## 3.2 In the joint space

From the constraint equations (1), by using the *IGM* (2) and the Cartesian coordinates (13) we can define the desired reference trajectory vector  $\mathbf{q}_a^d$  for the three active linear joint variables. Similarly from the velocity of the Cartesian coordinates (12), by using the *IKM* (3) and the inverse Jacobian matrix (4) we can define the desired joint velocity vector  $\dot{\mathbf{q}}_a^d$ . Finally from the acceleration of the Cartesian coordinates (11), by using the second order *IKM* (6) we can define the desired joint acceleration  $\ddot{\mathbf{q}}_a^d$ .

## 3.3 Control law the joint space

We have to design a control law in the joint space. Our strategy is to define a PID control law by using a simplified model of the dynamic behavior of *Orthoglide*. To simplify the dynamic model we make two assumptions. First the most part of the inertia seen by each rotary motor is due to the inertia moment of the drive chain. From this physical observation about the mechanical design of *Orthoglide* we consider for the simplified model an inertia matrix, which is a constant diagonal matrix. Secondly the two combined characteristics a high sampling frequency and great accuracy of each encoder sensor allow to obtain the joint active variables  $q_a$  and  $\dot{q}_a$  without any filter. It is then possible to design a feedback with high gain values. These high gain values allow to compensate the Coriolis, centrifugal, gravity, and friction effects, which are represented by the vector  $\mathbf{h}(\mathbf{q}, \dot{\mathbf{q}})$ . Therefore the simplified model is a decoupled two integrator model as follows :

$$\begin{pmatrix} d_{11} & 0 & 0 \\ 0 & d_{22} & 0 \\ 0 & 0 & d_{33} \end{pmatrix} \ddot{\mathbf{q}}_a = \Gamma, \quad (14)$$

where the desired behavior of the robot is such that  $\ddot{\mathbf{q}}_a = w(t)$  with :

$$w(t) = \ddot{\mathbf{q}}_a^d + \mathbf{K}_p(\mathbf{q}_a^d - \mathbf{q}_a) + \mathbf{K}_i \int_0^t (\mathbf{q}_a^d - \mathbf{q}_a) d\tau + \mathbf{K}_d(\dot{\mathbf{q}}_a^d - \dot{\mathbf{q}}_a). \quad (15)$$

Here the gain matrices  $\mathbf{K}_p$ ,  $\mathbf{K}_i$ , and  $\mathbf{K}_d$  are  $(3 \times 3)$  diagonal matrices. The numerical values of the diagonal elements of the matrix  ${}^0\mathbf{J}_p^\top \mathbf{A}(\mathbf{q}) {}^0\mathbf{J}_p$  are very close, due to the identical design of the three legs of *Orthoglide*. Therefore  $d_{ii}$ ,  $i = 1, 2$ , and  $3$  are set equal to the maximum modulus  $d_{max}$  of the diagonal elements of  ${}^0\mathbf{J}_p^\top \mathbf{A}(\mathbf{q}) {}^0\mathbf{J}_p$ . Therefore we can design for each active joint the same PID controller with the following scalar coefficients  $k_p$ ,  $k_i$ , and  $k_d$ . From  $\ddot{\mathbf{q}}_a = w(t)$  the introduction of the Laplace operator  $s$  yields for each joint :

$$(\mathbf{Q}(s) - \mathbf{Q}^d(s))(s^3 + k_d s^2 + k_p s + k_i) = 0 \quad (16)$$

Equation (16) can be written as follows :

$$(\mathbf{Q}(s) - \mathbf{Q}^d(s))[(s + \omega_n)(s^2 + 2\zeta\omega_n s + \omega_n^2)] = 0, \quad (17)$$

with  $k_d = (2\zeta + 1)\omega_n$ ,  $k_p = (2\zeta + 1)\omega_n^2$ , and  $k_i = \omega_n^3$ . By tuning  $\zeta = 1$  the controller gains are such that a transfer function is obtained with a real pole of multiplicity three, which is located in the complex left half plane. This means that (17) becomes :

$$(\mathbf{Q}(s) - \mathbf{Q}^d(s))(s + \omega_n)^3 = 0. \quad (18)$$

To obtain a feedback control in the joint space with a cut-off frequency ( $-3$  dB) equals to  $15$  Hz, we take  $\omega_n = 188$  rad/s to compute the gains  $k_p$ ,  $k_i$ , and  $k_d$ . This pulsation  $\omega_n$  is twice the pulsation corresponding to  $15$  Hz ( $94$  rad/s).

To summarize following the method of the computed torque the force vector  $\Gamma$  is computed through (14) substituting  $\ddot{\mathbf{q}}_a$  with  $w(t)$ .

## 4 Experimental results

A co-manipulation task over a period of  $30$  seconds is presented here. The operator moves the platform freely in the workspace, then at time  $t = 16.5$  s puts an additional  $4.11$  kg mass on the platform to test the robustness of the haptic control. Figure 2 presents the evolutions as function of time of the three actuator forces during the co-manipulation. The effect of the additional mass is observable through the vertical dashed line defining  $t = 16.5$  s. The jump of  $\Gamma_3$  acting following the vertical  $z$ -axis is almost equal to  $40$  N, that is coherent with the value  $4.11$  kg. There is also an effect on the force  $\Gamma_1$  and  $\Gamma_2$  acting along the  $x$ -axis and  $y$ -axis respectively. The measured forces by the force sensor are shown Figure 3. To avoid chattering effects on the measures around the value  $0$  N of the force sensor a thresholding of  $0.5$  N is taken into account. These profiles show that during the co-manipulation the experimenter has not to apply more efforts to move freely the platform, despite the addition of a  $4.11$  kg mass. A similar observation can be made from the coordinates of the Cartesian position of the platform,  $4.11$  kg mass does not affect the platform position, Figure 4. Let us remark that during the motion of the platform the magnitude of the tracking errors of the active linear joint variable does not exceed  $10^{-5}$  m. The strategy of focusing on the use of the reduced model (14) and the second-order system stabilization with PID feedback (15) rather than explicitly compensating for gravity is effective and has the advantage of being robust. Indeed, explicitly compensating for the effect of an additional mass requires knowing it a priori. These results prove that entire actuation chain, force and position sensors, acquisition cards and a well-defined control of active variables provide haptic control to perform a co-manipulation task that is comfortable for the human and accurate. To illustrate the quality of the co-manipulation task a video

was made during this experiment and it is in free access through this link :

[//uncloud.univ-nantes.fr/index.php/s/BjrYmceM3FnDzXc](https://uncloud.univ-nantes.fr/index.php/s/BjrYmceM3FnDzXc)

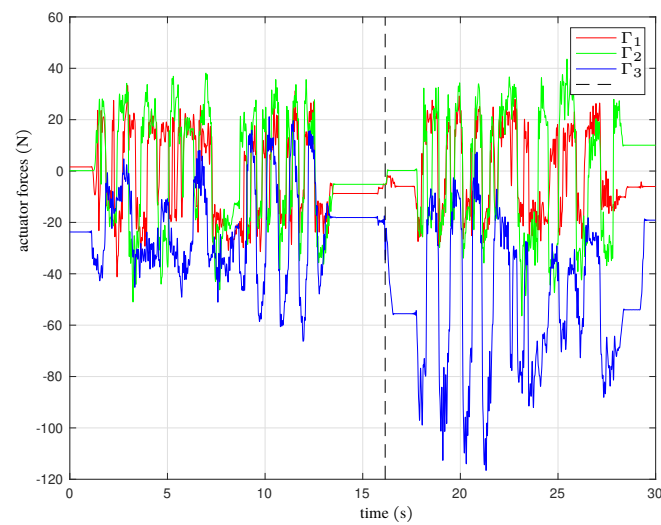


FIGURE 2: Profiles as function of time of the actuator forces during the experiment of co-manipulation of *Orthoglide*.

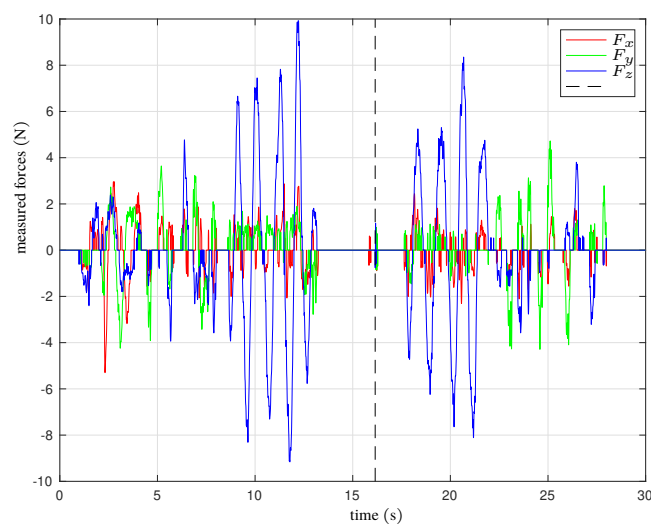


FIGURE 3: Profiles as function of time of the measured forces applied on the platform of *Orthoglide*.

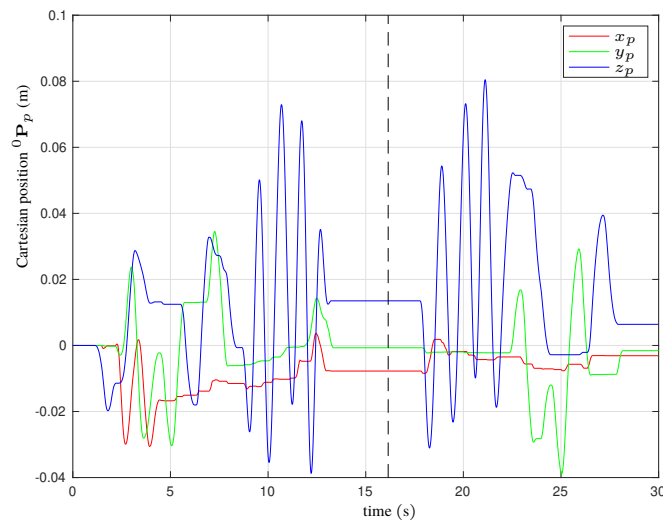


FIGURE 4: Profiles as function of time of the Cartesian position  ${}^0\mathbf{P}_p$  of the platform of *Orthoglide*.

## 5 Conclusion

In this paper we prove that it is possible to design a haptic feedback for a complex robot with closed structures, the parallel robot *Orthoglide*. Rigorous physics arguments make it possible to define a reduced linear model in order to take into account the dynamics of the robot *Orthoglide* in the control laws of the joint variables. Experimental results prove that thanks to high gain values of a feedback control based on a reduced model the reference trajectories of the active joints are perfectly tracked. Moreover, experimental tests show that the addition of a significant mass on the effector does not disturb the robot's behavior during a co-manipulation task. Similarly, an unexpected elastic or rigid contact of the effector with an obstacle does not cause unstable behavior of the robot. These experimental results prove that robust co-manipulation tasks can be performed with industrial robots without the need for costly specific adaptations. First our perspective is to extend our work to a six-axis serial robot. The displacement of the effector will be the result of a composition of rotational and translational movements. Secondly we want to investigate the teleoperation tasks, see [14]. Indeed *Orthoglide* has a little brother, the parallel robot *Orthoglide* five-axis, which is an evolution of the present *Orthoglide*, with two additional degrees of freedom on its effector, see [15].

## Références

- [1] W. Khalil, E. Dombre, Modeling, identification and control of robots, Butterworth Heinemann, 2002.
- [2] X. Li, G. Chi, S. Vidas, C. C. Cheah, Human-guided robotic co-manipulation : Two illustrative scenarios, *IEEE Trans. on Control Systems Technology* 24 (5) (2016) 1751–1763.
- [3] X. Lamy, F. Collédani, F. Geffard, Y. Measson, G. Morel, Overcoming human force amplification limitations in co-manipulation tasks with industrial robot, in : Proc. of the 8th World congress on Intelligent control and automation, Jinan, China, 2010, pp. 592–598.
- [4] L. Peternel, C. Fang, N. Tsagarakis, A. Ajoudani, Online human muscle force estimation for fatigue management in human-robot co-manipulation, in : Proc. of IEEE/RSJ Int. Conf. on Intelligent Robots and Systems (IROS), Madrid, Spain, 2018, pp. 1340–1346.
- [5] D. Chablat, P. Wenger, Architecture optimization of a 3-dof translational parallel for machining applications, the orthoglide, *IEEE Trans. on Robotics and Automation* 19 (3) (2003) 403–410.
- [6] D. Gorinevsky, A. Formalky, A. Schneider, Force control of robotics systems, CRC Press, first edition, 1997.
- [7] S. Devie, P. P. Robet, Y. Aoustin, M. Gautier, Impedance control using a cascaded loop force control, *IEEE Robotics and Automation Letters (RA-L)* 3 (13) (2018) 1537–1543.
- [8] F. A. L. Molina, J. M. M. Rosario, D. Dumur, P. Wenger, Application of predictive control techniques within parallel robot, *Sba Controle & Automação sociedade brasileira de automatica* 23 (5) (2012) 530–540.
- [9] Y. Xiong, F. Quek, Hand motion gesture frequency properties and multimodal discourse analysis, *Int. J. of Computer Vision* 69 (3) (2006) 353–371.
- [10] S. Devie, Commande hybride force-position d'un robot avec ou sans capteur d'effort externe, Phd Thesis, Nantes University, 2019.
- [11] S. Briot, M. Gautier, Global identification of joint drive gains and dynamic parameters of parallel robots, *Multibody System Dynamics* 33 (1) (2015) 3–26.
- [12] S. Guegan, W. Khalil, Dynamic modeling of the Orthoglide, Kluwer Academic Publishers, Caldes de Malavella, Spain, 2002, pp. 387–396.
- [13] S. Guegan, W. Khalil, P. Lemoine, Identification of the dynamic parameters of the orthoglide, in : Proc. IEEE Int. Conf. on Robotics & Automation, Taipei, Taiwan, 2003, pp. 14–19.
- [14] S. Devie, P. P. Robet, Y. Aoustin, M. Gautier, A cascade loop structure in force and position to control a bilateral teleoperation robotic system, in : Proc. of 6th Int. Conf. on Control, Decision and Information Technologies (CODIT'19), Paris, France, 2019.
- [15] R. Jha, D. Chablat, F. Rouillier, G. Moroz, Influence of the trajectory planning on the accuracy of the orthoglide 5-axis, in : Proc. of ASME 2016 International Design Engineering technical conferences & Computers and information in engineering conference, IDETC/CIE, Charlotte, North Carolina, 2016, pp. 1–9.